Powder Technology 273 (2015) 165–175

Contents lists available at ScienceDirect

Powder Technology

journal homepage: www.elsevier.com/locate/powtec

Investigation of coating layer morphology by micro-computed X-ray tomography

Franziska Sondej [a,1], Andreas Bück [a], Katharina Koslowsky [a], Philipp Bachmann [a], Michael Jacob [b], Evangelos Tsotsas [a]

[a] Thermal Process Engineering/NaWiTec, Otto-von-Guericke University Magdeburg, Universitätsplatz 2, 39106 Magdeburg, Germany
[b] Glatt Ingenieurtechnik GmbH, Nordstraße 12, 99427 Weimar, Germany

ARTICLE INFO

Article history:
Received 12 June 2014
Received in revised form 23 December 2014
Accepted 28 December 2014
Available online 5 January 2015

Keywords:
Spray fluidized bed coating
Layer morphology
Layer thickness
Porosity
Micro-computed X-ray tomography

ABSTRACT

Spray fluidized bed coating is a common process in food, chemical and pharmaceutical industry. Morphology of the formed layer is essential for product quality. Therefore, layer morphology was investigated in detail by X-ray micro-computed tomography (μ-CT) for porous γ-alumina particles coated with a solution of sodium benzoate with some hydroxypropyl-methylcellulose in water. Investigated properties are: layer thickness distribution on individual particles, porosity of the layer, and average layer thickness. The determination of layer thickness was performed in two different ways: (1) using two-dimensional cross-sections of volume images obtained from full μ-CT measurements, and (2) using single X-ray irradiation images without sample rotation. The porosity of the coating layer was evaluated from the volume images. Further studies were performed to investigate the influence of operating parameter, e.g. exposure time, on image quality and the obtained results. Special attention was put on ways to reduce the necessary measurement time while preserving the quality of the results. Finally, a new measurement protocol is presented which allows to measure coating thickness distributions in a particle population.

1. Introduction

Coating of particles is widely used in the chemical, agrochemical, pharmaceutical and food industry to obtain products with required end-user functionalities [1], for instance odor or taste masking, protection from environmental influences, improved flow ability or the controlled release of an active substance [2]. The general idea of coating is shown in Fig. 1: Core particles, e.g. an active pharmaceutical ingredient, are sprayed with a coating solution containing a solid different from the core material. The droplets spread on the surface of the particle building up a film. The solvent, i.e. the liquid portion of the solution, is generally evaporated, and a solid layer is formed on the particle surface. The main aim of this process is not to achieve a large increase in particle size, as for instance in layering granulation, but to functionalize the core particle. The aforementioned functionalities depend strongly on the characteristics of the coating layer, e.g. layer thickness, coating porosity, coating uniformity or microstructure, so in order to guarantee the product quality of coated particles, a precise characterization and identification of the quality of the layers is necessary, as well as a correlation to the operating conditions of the layer formation process.

Basic techniques, commonly applied for characterization of the quality of coating layers on particles are light microscopy or scanning electron microscopy (SEM). Starting in the 1990s, coated particles were investigated, for example by cutting them in their equatorial plane and then examining the cut by SEM, see, e.g., [3]. Andersson et al. [4] also cut coated particles, took images with a fluorescence microscope and evaluated these using image processing algorithms. However, these methods of characterization are either cumbersome to apply and destructive, or they provide information restricted to the sample surface. When destructively applied, sample preparation, like cutting the particle or scraping the coating layer, may distort the results. Moreover, optically similar materials may be hard to distinguish and separate from each other, and quantitative evaluation of the images is difficult.

In 2009, confocal laser scanning microscopy (CLSM) was presented by Laksmana et al. [5] as a non-destructive method for the determination of coating thickness. These authors analyzed the layer thickness distribution on single particles, as well as layer porosity and pore size distribution of granules coated with HPMC. Depypere et al. [6] investigated small primary particles ($d \approx 200$ μm) with very thin coating layers ($s < 5$ μm) also by CLSM. The resulting images were analyzed by image processing with regard to the layer thickness distribution on single particles. Cahyadi et al. [7] used the destructive version of light microscopy to calibrate non-destructive measurements of layer thickness by Raman spectroscopy, infrared spectroscopy and X-ray fluorescence analysis. Sasic [8] used Fourier transform infrared microscopy to determine the film thickness on tablets. In order to be able to do so,

E-mail address: franziska.sondej@ovgu.de (F. Sondej).
[1] Tel.: +49 391 6712320; fax: +49 391 6718265.

http://dx.doi.org/10.1016/j.powtec.2014.12.050
0032-5910/

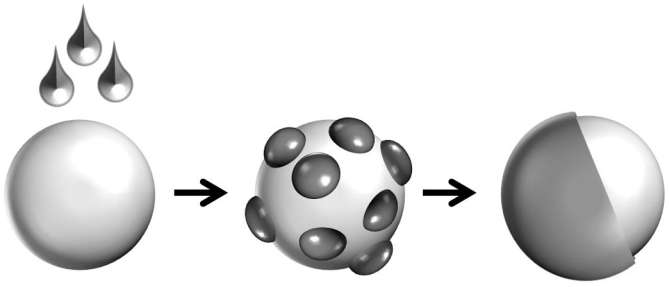

Fig. 1. Coating scheme.

the tablets had to be split before the measurement. Koller et al. [9] as well as Zhong et al. [10] applied optical coherence tomography as a further non-destructive method to determine coating thickness. Zhong et al. [10] and Russe et al. [11] used Terahertz pulsed imaging (TPI) for measurement of layer thickness. Special about this work is the application of micro-computed tomography to calibrate the TPI measurement device.

In this study, X-ray μ-computed tomography (μ-CT) is used as a technique for investigating and describing quantitatively the morphology of coating layers. The μ-CT is a method for non-destructive analysis of objects, e.g. coated particles, and provides information on the internal structure like layer thickness and micro-porosity. Using this system for the analysis of tablets or coating layers is a relatively new method, which has only been the topic in a few publications so far. The μ-computed tomography was used for the first time in 2003 by Farber et al. [12] who tried to get information about the porosity and the pore size distribution of pharmaceutical granules. Hancock et al. [13] and Zeitler et al. [14] provided an overview of dosage forms which were analyzed by μ-CT.

The first investigation of coating layers with μ-CT was performed by Perfetti et al. [15], who determined characteristics of the coating layer such as porosity and layer thickness. By principle, X-ray μ-computed tomography is not restricted to the investigation of coating layers but can also be applied to reveal the inner morphology of agglomerates. In Dadkhah et al. [16], agglomerates which were produced in a fluidized bed were evaluated using μ-CT. Different types of image analysis operations were applied in order to get information from the μ-CT images, such as the number of primary particles, the fractal dimension of the formed agglomerates and other morphological descriptors that influence the product quality, for example the mean coordination number of primary particles, i.e. the mean number of connections of one primary particle to other surrounding primary particles, which strongly influences the strength of the formed agglomerate.

The present investigation aims at contributing to a better characterization of coated particles using X-ray μ-CT. The performance of the methodology will be assessed by variation of μ-CT operating parameters. Furthermore, a novel protocol will be developed for determining coating layer thickness and layer porosity of particles produced in a spray fluidized bed. Another issue that will be discussed in this study is the minimum time required for μ-CT measurements of the coating layer thickness, and an alternative approach to obtain this information will be presented. Finally, it will be shown and discussed how μ-CT measurements can be performed to obtain not only information on the layer thickness of individual particles but also on the layer thickness distribution in a particle population.

2. Materials and methods

2.1. Particle coating process

The particle coating was realized in a lab-scale batch fluidized bed granulator with a cylindrical fluidization chamber with 150 mm internal diameter and a height of 450 mm (type WSA 150, Glatt Ingenieurtechnik GmbH, Weimar, Germany). A schematic of the experimental setup is shown in Fig. 2. The coating solution was sprayed in batch operation using a two-fluid nozzle (model 940, Düsen Schlick GmbH, Germany), which was placed in bottom spray configuration. The nozzle parameters were chosen such that the average droplet diameter is approximately 40 μm. Droplets were sprayed in a Wurster tube with an inner diameter of 70 mm and a height of 200 mm, placed at a distance of 20 mm from the air distributor plate. It should be noted that bottom-spray Wurster equipment is widely used in practice for coating, because of flow patterns that help to avoid agglomeration and rather uniformly distributed circulation times of particles that promote uniform coating [17]. All process parameters such as spraying rate, fluidization air flow rate and gas inlet gas temperature were kept constant during the experiments.

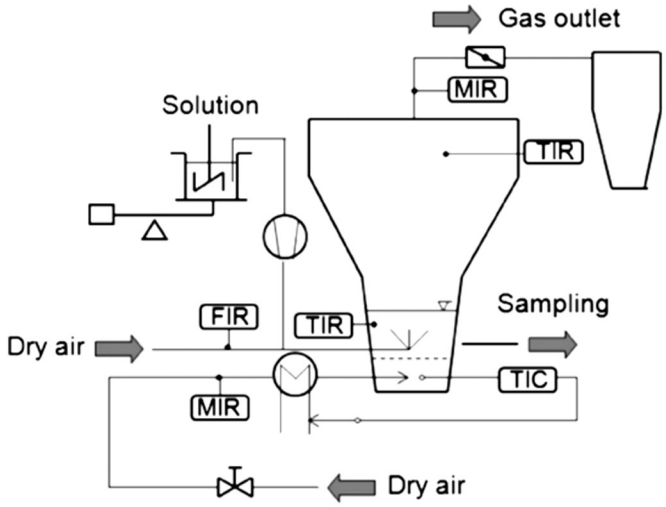

Fig. 2. Experimental setup of the lab-scale fluidized bed, (TIC/TIR temperature indicate controller and recorder, MIR/FIR mass and fluid indicate recorder).

Porous γ-Al_2O_3 beads (Sasol GmbH, Germany) with an average diameter of 1.8 mm were used as core particles. The γ-type of Al_2O_3 is a common material for granulation studies with porous particles, because it can readily be purchased at constant quality, is stable towards mechanical and thermal stresses and has a very high sphericity (0.983), which is an important advantage for fundamentally oriented investigations. Right before the coating experiments were started, the particle size distribution of the core material was measured using a Camsizer (Retsch GmbH, Haan, Germany). Based on image analysis, the device also determines the (mean) sphericity of the measured particles. The core particles were coated with a solution consisting of sodium benzoate (NaB, 28.5 mass-%) and hydroxypropyl methylcellulose (HPMC, 0.3 mass-%) as the solutes, and demineralized water as the solvent. Sodium benzoate (Trigon Chemie GmbH) is an antifungal agent used as a preservative in many industrial sectors. Furthermore, the salt has a good solubility in water, so that a mass fraction of approximately 30% can be achieved under room conditions. The solution also contains HPMC (Pharmacoat 606, Shin-Etsu, Japan), which finds widespread application as coating material or binder in the food and the pharmaceutical industry because of its good film-forming and adhesive properties. HPMC has been used in this work to promote the uniformity of coating. All relevant properties of the solid materials are summarized in Table 1.

Table 1
Solid material properties.

Parameter	Value
Density γ-Al_2O_3 beads	1040 kg/m^3
Average diameter of γ-Al_2O_3 beads	1.8 mm
Density of solid sodium benzoate	1440 kg/m^3
Density of solid HPMC	1310 kg/m^3

For the coating process, the spraying rate was set to 600 g/h, the gas inlet temperature to 60 °C and the pressure of the nozzle to 1 bar. The initial bed mass of core particles was 1000 g. The coating process was performed for 1 hour, which corresponds to a final particle mass of 1180 g. All relevant parameters are summarized in Table 2.

2.2. Principles of X-ray μ-computed tomography

The main principle of X-ray μ-computed tomography is depicted in Fig. 3. The object to be investigated is placed on a sample holder in the beam cone created by the X-rays emitted from the X-ray source and collected on the detector. The sample holder is rotating around its z-axis with an adjustable speed or angular increment. After each increment the X-rays passing the sample and hitting the detector plane create on the collector intensity profiles, which can be visualized as a set of gray-scale values, so that after a full revolution a set of two-dimensional sectional representations of the sample under different angles are available. By tomographic reconstruction techniques a three-dimensional volume image can be created from the series of two-dimensional intensity matrices. Due to the different X-ray absorption capacity of the materials in and on the particles and the surrounding, the different phases (core material, coating material and air) can be separated via the local absorption per volume element (voxel). The minimum voxel size (a volume) determines the spatial resolution, i.e. the size of the smallest geometric quantity that can be resolved. The inner morphology of the core particle and the coating layer can then be investigated based on the tomographic reconstruction, and it is possible to examine the particle non-destructively, i.e. measurements can be repeated on one and the same particle [18].

In this study, the coated particles, which require no pre-treatment other than fixing each of them to the sample holder, were scanned utilizing a customized X-ray μ-computed tomographic device (CT Procon alpha 2000 by ProCon X-ray GmbH, Garbsen, Germany). This device is equipped with a micro-focus X-ray source and has a detector size of 100 × 100 mm^2 or 2304 × 2304 pixels. The software Volex (Fraunhofer Institute for Integrated Circuits, IIS, Erlangen, Germany) was used for measurement and reconstruction of the volumetric images. In image acquisition the adjustment of brightness and contrast is important, which is done by setting voltage and current of the X-ray tube. The sample holder was placed as close as possible to the X-ray source, approximately 400 mm from the detector. The distance of sample holder and detector determines the magnification of the system [15]. The samples should stick on the sample holder firmly, because every movement of the sample during rotation will otherwise yield blurred volume images. The distance of the detector to the tube was kept constant for all measurements. By rotation of the sample holder, the particles were scanned in the entire range from 0 to 360°. Operating parameters of the X-ray source like voltage (50 kV), current (170 μA), and the exposure time (2000 ms) were kept constant for all measurement because these parameters ensure high-quality X-ray images. Other parameters such as rotation step, i.e. the angular increment, and averaging (number of taken images for one angle) with skip (number of images which are discarded per one record) can be varied to obtain high-quality volume images fast.

Table 2
Process parameters.

Parameter	Value
Gas inlet temperature	60 °C
Spraying rate (liquid and solid)	600 g/h
Solid concentration of sodium benzoate in solution	28.5 mass-%
Solid concentration of HPMC in solution	0.3 mass-%
Fluidization gas flow rate	160 m^3/h
Initial bed mass	1000 g
Process duration	1 h

3. Image analysis and evaluation

3.1. Image processing

Image processing employs methods for improvement of pictorial information for human perception, for example contrast enhancement, de-blurring and procedures for the extraction of image information suitable for further processing. Typical tasks are, among others, object counting, object measurement and object identification. In μ-CT measurements, an image consists of a digitized array of different gray values representing intensities or local absorption values, which are obtained from the detector. The main task of the image analysis is then to extract the inner structure of the scanned sample, e.g. the layer thickness and porosity. For this some initial image processing is necessary to improve the image quality and to enhance the visibility of the different constituents [19]. In this study, the protocol established in Dadkhah et al. [16] has been followed.

The determination of the coating thickness on a single particle was conducted in two different ways: (1) using volume images which were obtained after a complete μ-CT measurement (one full revolution of the sample) and (2) using single two-dimensional images (fixed angular position). The volume images were analyzed with the software Volume Player Plus (Fraunhofer Development Center for X-ray Technology, Germany). To improve the visualization of the layer, an adjustment of contrast and brightness was performed. Attention should be paid to the fact that this step in image processing is subjective, depending on the individually perceived image quality and resolution. A two-dimensional image which shows the equatorial plane was chosen for the evaluation; an example is depicted in Fig. 4. In both measurement ways, the images were saved, and the voxel size (number of pixels in a two-dimensional image: 1.5 to 1.7) was noted.

The coating thickness was determined for both measuring methods in the same way utilizing the software ImageJ (National Institutes of Health, USA). The image processing of the obtained projection slices (two-dimensional images) consists of the following steps: cropping the region of interest, image binarization, separation of the inner constituent due to the different density and X-ray absorption of core and layer, and application of a suitable filter to fill the voids in the coating layer in case of measuring the layer thickness only.

In order to measure the coating layer thickness, the equatorial plane of the spherical particle must be determined as otherwise only a layer chord-length is measured. The equatorial plane of the spherical particle is determined indirectly: After the μCT measurement, a set of two-dimensional slices is available on which the core particle can be clearly distinguished from the coating material. This also allows measuring the cord-length of the core particle in each slice (automatically by the image processing software). The equatorial plane is chosen as the plane where the cord-length assumes its maximum. The error in the chord-length of the core particle is in the order of the measurement resolution, i.e. approximately 2 μm. Compared to the actual diameter of the particle of 1800 μm, this error is negligible, and also the error in the determination of the coating layer is very small.

For determination of the coating layer thickness a circle was defined which has the same center point as the particle. The perimeter has to enclose the entire particle together with the coating layer. The ImageJ application “Radial Grid” places a grid over the measuring region with radially extending straight lines. Along these radial lines the thickness of the coating layer can be determined by detection of the black and white boundaries. The processing steps are shown for one particle in Figs. 5 and 6. The measurement angles were selected manually, so that certain subjectivity is present in the obtained results.

The porosity of the coating layer was processed and analyzed with the MAVI software (Fraunhofer Institute for Technical and Industrial Mathematics, Kaiserslautern, Germany). The first steps are similar to the steps of the evaluation of coating thickness from the volume images: cropping the region of interest, removing measurement noise by

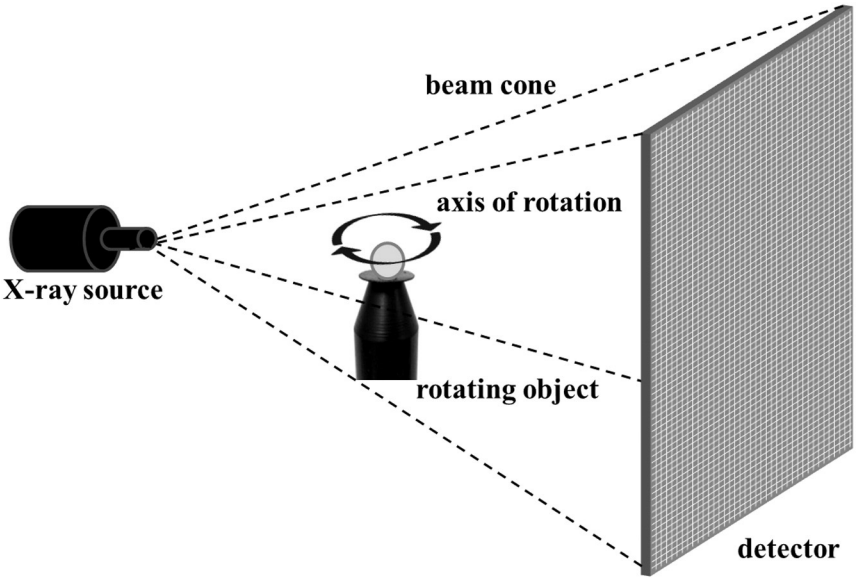

Fig. 3. Principle of μ-computed tomography.

filtering and image binarization. The software calculates the volume of the binarized coating layer (V_F), excluding all existing voids by counting the voxels. The morphological transformation operator "closing" was used to close all internal voids. Only pixels that belong to the layer, which can be determined from the different gray values of core particle and coating material, were taken into account for the porosity calculation. The volume was calculated a second time for the layer with filled voids (V), shown in Fig. 7. From this information and Eq. (2) in the next section, the shell porosity can be determined.

3.2. Calculation of coating thickness and porosity

In two-dimensional setting, the thickness of the coating layer (or the shell thickness) *s* can be expressed simply by the difference of outer radius of the coating layer and the radius of the core particle. In Fig. 8 the situation of a non-spherical core particle with a non-uniform coating layer is depicted. Then the layer thickness varies spatially, which can be expressed in terms of the angle α:

$$s(\alpha) = r_{cs}(\alpha) - r_c(\alpha), \qquad \alpha \in [0,\ 360^\circ)$$

The origin for the radius measurement has to be placed inside the core particle, for instance at the center of gravity. Note that in case of an ideal spherical core particle with a perfect coating, i.e. when the particle remains ideally spherical after coating, no angular dependency exists and the shell thickness can also be expressed in terms of the difference of measured diameters.

In a three-dimensional setting, the definition of shell thickness has to be extended by one more angle, e.g. β, and the local shell thickness can then be expressed similarly:

$$s(\alpha,\beta) = r_{cs}(\alpha,\beta) - r_c(\alpha,\beta), \qquad \alpha \in [0,\ 360^\circ),\ \ \beta \in [0,\ 180^\circ]$$

This definition again allows for local deviations from the spherical shape in both, the core and the coated particle.

The direct calculation of the local shell thickness is a classical inverse problem and can only be solved for special cases, e.g. for the case of ideally spherical core particles with an ideally uniform coating with uniform shell porosity. For this case, with known total mass of coating dry matter (M_c) added to the bed and total mass of core particles in the bed (M_p), Depypere et al. [6] presented an equation to calculate the theoretical layer thickness

$$s = \frac{d_p}{2}\left[\left(1 + \frac{\rho_p \cdot M_c}{(1-\varepsilon_c)\rho_s \cdot M_p}\right)^{1/3} - 1\right] \tag{1}$$

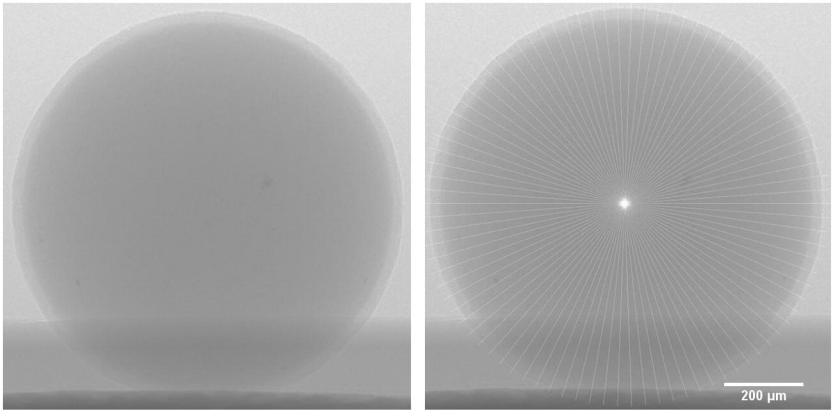

Fig. 4. X-ray image of a coated alumina particle; right: with radial grid.

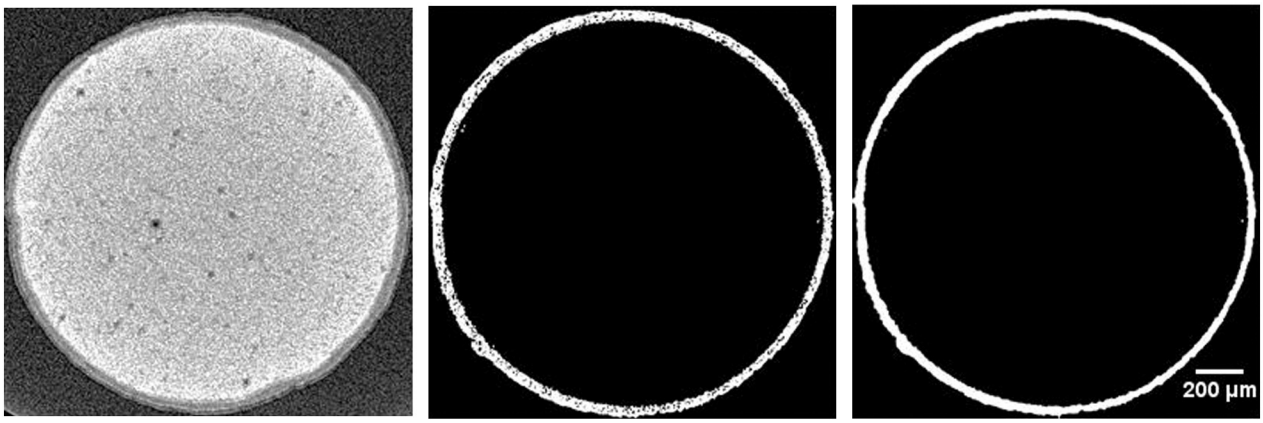

Fig. 5. Coating layer: binarized, separated, filled with closing operator.

In this equation, the particle density of the core particles is given by ρ_p, whereas ρ_s is the solid density of the coating material. Due to thermal effects during drying, the coating layer will not be completely compact but possess certain porosity. The mean porosity of the coating layer (ε_c) depends on the composition of coating materials and on the chosen parameters in the coating process.

For evaluating the layer porosity, and knowing the image voxel size, the mathematical morphology operator "closing" was used to close all internal voids, as described before. The mean porosity of the coating layer can be calculated based on the values obtained from the described volume analysis:

$$\varepsilon_c = 1 - \frac{V_F}{V}, \tag{2}$$

where V_F is the volume of the coating layer excluding voids and V is the layer volume after closing.

4. Results and discussion

4.1. Evaluation of coating uniformity

As mentioned before, µ-CT measurements provide a variety of information about the inner structure of core particle and coating layer. For an assessment of the quality of the obtained images, a series of µ-CT measurements were performed on one and the same coated particle varying image averaging and skipping, and also rotation steps. Operating parameters kept constant in these measurements are listed in Table 3. Varied operating parameters and results are summarized in Table 4. For the images obtained in measurements B1 to B4, no averaging was performed. The measurements C1 to C4 were conducted by automatically taking three images per angle, skipping one of them based on the worst quality (internally determined by the software) and generating an average image from the remaining two.

First, the uniformity of the formed coating layer shall be discussed. To this purpose, the radial distributions of coating thickness obtained from measurements B1 and C1 are shown in Fig. 9. Tube settings and rotation steps were constant, so that these two evaluations differ only in the use, or not, of image averaging. All thicknesses are in the range from 42.5 µm to 56.3 µm, cf. Fig. 10. Measurement B1 delivered a mean coating thickness of 48.1 µm and a standard deviation of 3.08 µm. From measurement C1 a mean layer thickness of 47.8 µm and a standard deviation of 2.61 µm were obtained. As mentioned before, the positions for the evaluation of the layer thickness distribution were selected manually, corresponding to a limited number of values on the abscissa of Fig. 9. No indication of a correlation with the measuring angle is discernible in Fig. 9, meaning that coating layer thickness is randomly distributed over the angular position. Stripe plots for other pairs of measurements are not shown here, but they support this conclusion.

The measurements B2 and C2 differ also in the setting of image averaging, and in a larger step of rotation compared to B1 and C1. Both measurements deliver the same mean thickness of 48.2 µm and an almost identical standard deviation of 2.66 µm for B2 and 2.46 µm for C2. The range of values, from 42.5 µm to 54.0 µm, is almost the same to the range of thicknesses of measurements B1 and C1.

In measurements B3 and C3 the angular increment was increased further to 0.45°, otherwise B3 and C3 differ in the setting of image averaging. The measured thicknesses range from 43.2 to 54.8 µm. Measurement B3 delivered a mean coating thickness of 48.3 µm and a

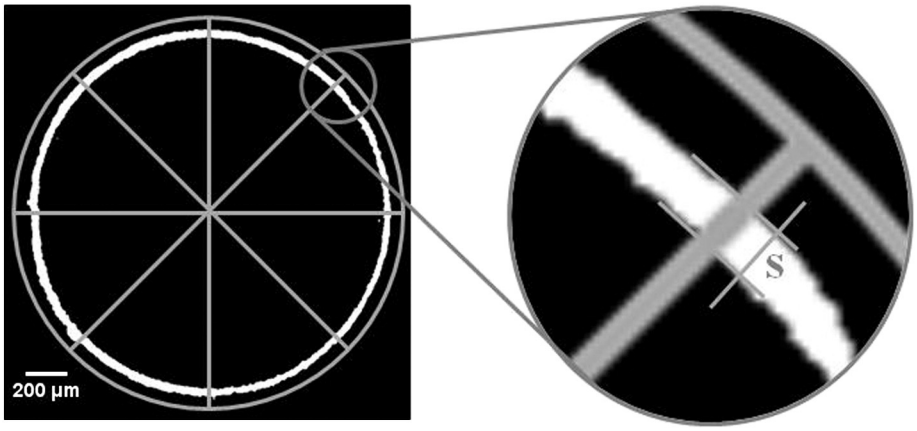

Fig. 6. Detailed illustration of the use of the radial grid to obtain layer thicknesses.

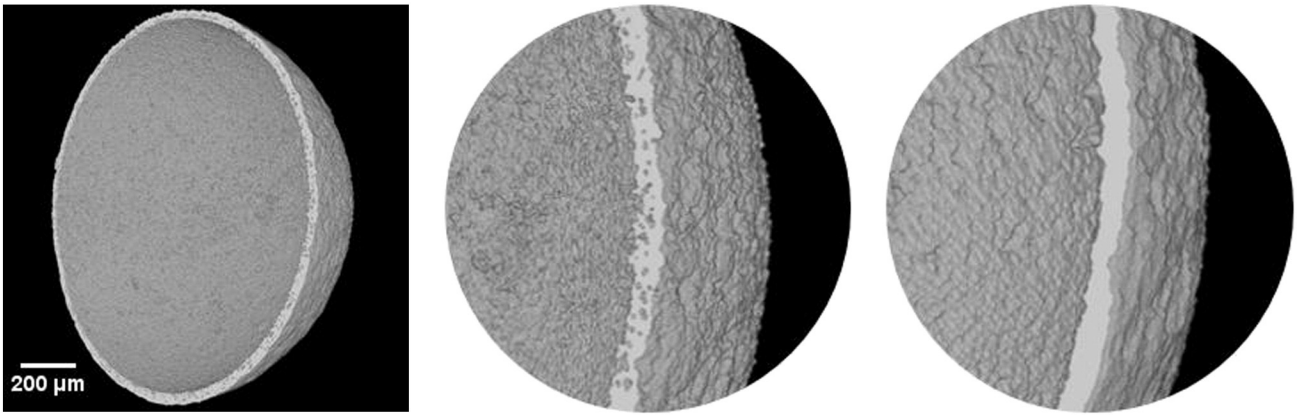

Fig. 7. Separated coating layer, filled with "closing" operator.

standard deviation of 2.34 µm whereas from measurement C3 a mean layer thickness of 48.5 µm and a standard deviation of 2.48 µm were obtained.

Measurements B4 and C4 were done with the highest rotation step of 0.9°. Thicknesses are in the range from 43.4 µm to 52.0 µm. However, these two measurements deliver mean thickness values which are furthest apart from each other. From experiment B4 a mean thickness of 48.3 µm with a standard deviation of 1.8 µ were obtained. Experiment C4 delivers 47.6 µm and 2.8 µm, respectively.

Fig. 10 presents the cumulative frequency distributions of all obtained local coating thickness values for measurements B1 to C4. All distributions are of similar shape to normal distributions. The range of the s_{50}-values is from 47.0 µm to 49.8 µm. The mean s_{50}-value is 48.5 µm. The non-smooth appearance of the curves is due to failing availability of measurement data for certain angles, e.g. from 135° to 225°. This is the range of angles covering the part of the particle which was fixed on the sample holder (cf. Fig. 4). These parts are difficult to resolve, due to similar gray values between particle and sample holder surface.

4.2. µ-CT measurements for evaluation of mean coating thickness and mean coating porosity

Figs. 11 and 12 show the difference between averaged and non-averaged µ-CT recordings. The image on the left-hand side (Fig. 11) seems to be sharp but coarse-grained. The edge of the coating layer is hard to identify due to measurement noise; additionally the exterior of the coated particle is not uniformly black. The image on the right-hand side (Fig. 12) appears smoother. The transitions between core particle and coating layer and between coating layer and environment are smoother and clearer. Errors in the recorded images, e.g. noise, are compensated or deleted by averaging. Nevertheless, all values of average coating thickness lie in Table 4 in a narrow range from 47.6 µm to 48.5 µm. This means that averaging may improve image quality, but it does not pay off in terms of accuracy in the determination of average coating thickness, because the latter does not vary significantly, whereas measuring time is increased compared to the measuring time without averaging by a factor of approximately two. The same holds in regard of smaller rotation steps. Consequently, the data of Table 4 indicate that µ-CT measurements result in a sufficiently accurate determination of mean coating thickness even with large rotation steps for the investigated combination of materials. For these materials, the differences in gray values between core particle and coating layer and between environment and coating layer appear to be high enough for separating the phases properly and evaluating the thickness of the coating layer accurately. The thickness difference between measurements B1 and C1 was around 0.3 µm (0.62%). For B2 and C2 no difference was observed, whereas the difference between B3 and C3 was 0.2 µm (0.21%). The difference in the average thickness was largest between B4 and C4 with a value of 0.7 µm, which is only slightly above the maximum resolution of the used µ-CT device (0.6 µm) and gives an estimate of the influence of the averaging operation on the measured layer thickness. The theoretical average thickness according to Eq. (1) would be 37.0 µm for a compact coating layer ($\varepsilon_c = 0$). However, as shown in Table 4, the evaluated average porosity of the coating layer is about $\varepsilon_c = 0.15$. If this porosity is considered in Eq. (1) the theoretical thickness increases to 47.6 µm and lies in the range of the experimentally determined thicknesses. Calculation with Eq. (1) indicates the consistency of the applied methods and the obtained results, but it is also prone to mistakes and limitations that will be briefly discussed in the following.

The results concerning the porosity of the coating layer are also summarized in Table 4. Independent of image averaging, the detected porosity was found to increase with an increase in rotation step, so that the lowest porosities were detected for measurements B1 and C1 with a rotation step of 0.225° and the highest for measurements B4 and C4 with the highest rotation step of 0.9°. Results with a large rotation step may suffer by the fact that the fewer projections have been recorded, the more difficult it is to set the threshold of gray values for the coating layer. At the other limit, a small rotation step means many projections and a high measuring time, which may lead to some wear and drift of the X-ray tube during

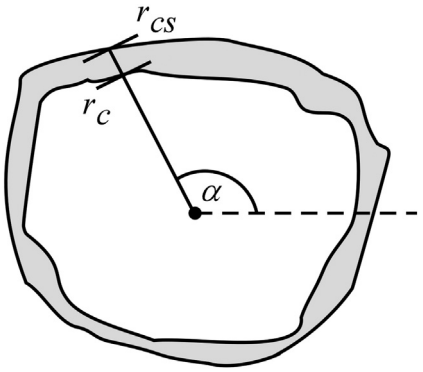

Fig. 8. Definition of shell/layer thickness (two-dimensional setup).

Table 3
Constant measurement setting.

Parameter	Value
Voltage	50 kV
Current	170 µA
Exposure time	2000 ms

Table 4
Results of the measurements for the investigation of coating thickness and porosity, depending on averaging and rotation steps.

Complete measurements	Averaging [−]	Skip [−]	Rotation steps [°]	Measurement Time [hh:mm]	Voxel size [μm/px]	Average thickness [μm]	Average porosity [−]	Standard deviation of coating thickness [μm]
B1	1	0	0.225	01:45	1.5	48.1	0.08	3.08
C1	3	1	0.225	03:30	1.5	47.8	0.15	2.61
B2	1	0	0.3	01:20	1.6	48.2	0.12	2.66
C2	3	1	0.3	02:40	1.6	48.2	0.17	2.46
B3	1	0	0.45	00:55	1.3	48.3	0.15	2.34
C3	3	1	0.45	01:44	1.3	48.5	0.18	2.48
B4	1	0	0.9	00:25	1.6	48.3	0.16	1.79
C4	3	1	0.9	00:53	1.6	47.6	0.19	2.81

the measurement. As mentioned before, the transition between core particle and coating layer is more difficult to identify, and phaseseparation is more difficult to perform without averaging, which appears to result in somewhat smaller values of detected porosity.

Eq. (1) can also be used to calculate a theoretical mean shell porosity if the mean layer thickness is given. Inserting the measured thickness of approximately 48 μm gives then a theoretical mean porosity of 0.18. This is slightly larger than the porosity of 0.15 that can be obtained by averaging the eight detected porosity values of Table 4, but still within the range of directly measured porosities. Despite the success of this comparison, as well as of the previously conducted inverse operation of calculating mean layer thickness from given mean coating porosity, it should not be overseen that application of Eq. (1) can be erroneous when the particles are not ideally spherical, the coating layer is not uniform, the porosity of the coating is not uniformly distributed in space, or some coating mass penetrates into porous core particles. Moreover, Eq. (1) has been applied in the present work by using the total coating mass and the total mass of cores in the fluidized bed. It should be noted that application of Eq. (1) can be upgraded by using instead of total masses the individual mass of coating on a specific core particle in combination with the individual mass and diameter of this core particle. This approach has been successfully practiced in [20], but it is quite laborious, because it requires determination of the weight and diameter of the coated particle, then removal of the coating by, e.g., dissolution, and finally determination of the weight and diameter of the core. And, it is still subjected to the serious restriction of particles being nearly spherical.

A conspicuousness seen in Table 4 is that the voxel size was not exactly the same for all measurements. The main reason for the variation of this value is differences in the distance from tube to sample. Initially, it has been tried to place the particle centrally on the sample holder for every experiment. However, placement was not always precise enough, resulting in some eccentricity of the particle, which then moves circularly by the rotation movement of the sample holder with the danger of leaving the field of vision. This effect has been compensated by increasing the distance from tube to sample.

4.3. Influence of HPMC on coating porosity

The obtained porosities, shown in Table 4, are all quite low signalizing an almost compact layer. This can be attributed to the HPMC present in the coating solution. During heating (in the experiment) the consistency of the binder becomes gel-like; after a cooling phase the binder solidifies [18]. The coating solution consists of initially dissolved sodium benzoate and HPMC. During the spraying process the dissolved substances unite due to HPMC becoming gel-like. The molecules of HPMC control the crystallization process of the sodium benzoate during the drying. As a result, the coating layer is rather compact; the crystals are agglutinated with the HPMC. Fig. 13 shows a SEM image of an investigated particle. In comparison, Hoffmann et al. [21], Rieck et al. [22] used sodium benzoate only (30 mass-%) as coating material. Although the process conditions were similar, the determined porosities were up to 50% larger than the results obtained using HPMC. Furthermore, the surface of the coating layer was uneven and fissured, Rieck et al. [22]. It can be conjured that film-forming substances have a large influence not only on the surface structure for which they are primarily used, but also on the porosity of coating layers and thus may have an influence on the product properties of coated particles such as the release rate or the behavior of dissolution. An experimental validation, however, has to be done in an independent study.

The use of spherical core particles and the addition of HPMC to the coating solution ensure that the obtained coated particles are almost ideally spherical with an almost homogeneous and quite compact coating layer. Due to this fact, results from the measurements are similar to the calculated thicknesses and porosities.

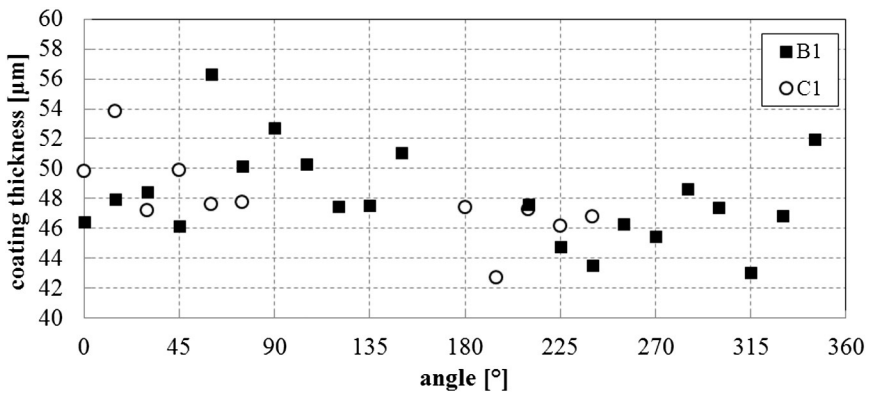

Fig. 9. Distribution of coating thickness for measurements B1 and C1.

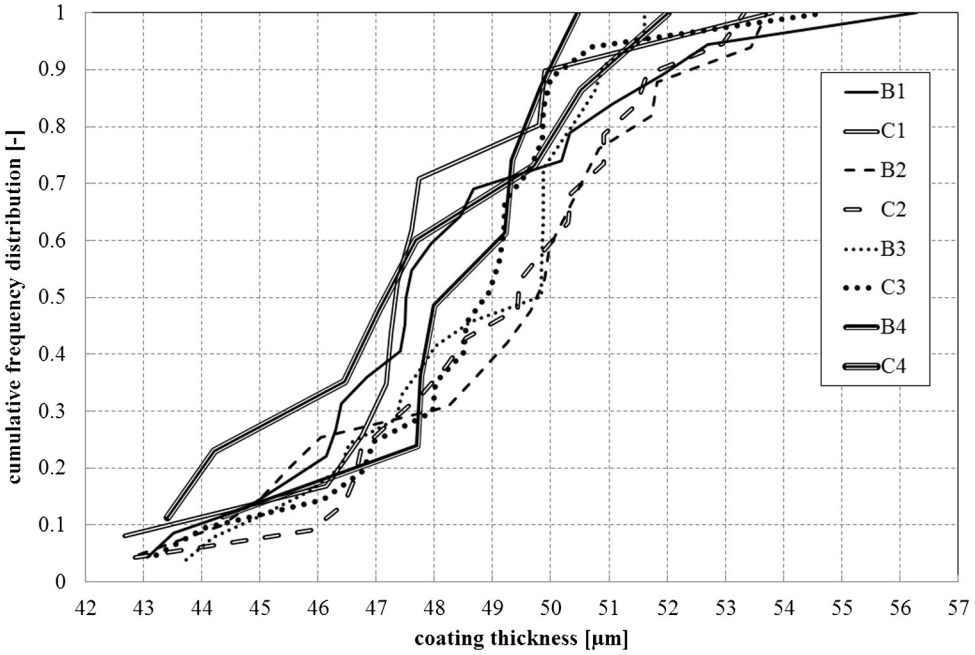

Fig. 10. Cumulative frequency distributions of coating thickness on a single particle.

4.4. Investigation of average coating thickness by single X-ray image and µ-CT measurement

The measurement procedure described so far was complex and very time-consuming. It will be discussed in this section how the time consumption and the complexity can be significantly reduced if only the layer thickness distribution is of interest.

Motivated by the results for the average layer thickness obtained from experiments C1 and C4 (Table 4) which were almost equal, but whereas experiment C1 took three and a half hours C4 took less than one hour due to the larger angular increment, the following extreme case was considered: A particle chosen randomly from the batch spray fluidized bed experiment (another particle than in case of Table 4) was placed onto the sample holder in the µ-CT. Then, using the operating parameters given in Table 3, a single X-ray image of the fixed particle was taken without any rotation of the sample.

This X-ray image was then analyzed with respect to the layer thickness after an adjustment of the brightness and contrast of the image. The coating layer could be distinguished easily from the core particle due to the differences in the densities and X-ray absorption behavior of the materials. The layer thickness was then evaluated at eight different positions evenly distributed along the particle circumference. The manually analyzed average thickness of the X-ray image was found to be 44.5 µm; the time necessary to obtain the image (including adjustment of brightness and contrast) was approximately two minutes. In order to assess whether this extreme case gives accurate information on the average layer thickness, complete µ-CT measurements with different angular increments but otherwise identical operating parameters were conducted for the same particle. The resulting volume images were evaluated in the same way as for measurements B1 to C4. In Table 5 the measured average layer thicknesses are shown, and it can be seen that they are almost equal.

However, the measuring time varies significantly with the number of rotation steps. With increasing number of rotation steps, i.e. decreasing angular increment, the necessary measuring time increases, in this case from two minutes up to almost two hours. In summary, the investigation of average coating thicknesses based on a single X-ray image is quick and uncomplicated but nevertheless quite precise compared to a fully-fledged µ-CT measurement. It should be noticed that the single X-ray image contains too much noise for layer porosity to be determined from it. However, Eq. (1) can still be used, resulting

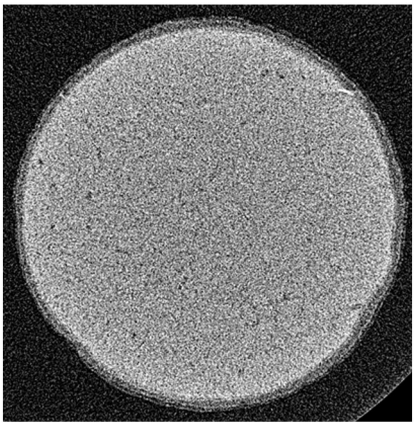

Fig. 11. Image recorded with rotation step 0.9° and no image averaging.

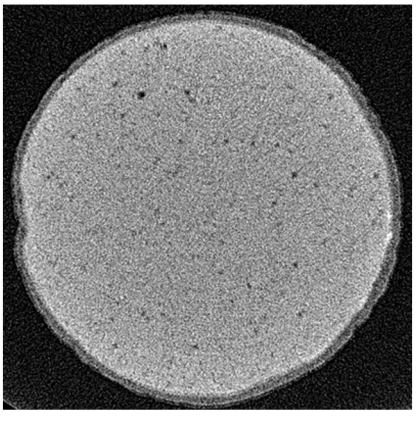

Fig. 12. Image recorded with rotation step 0.9° and an image averaging of 3 and 1 image skipped.

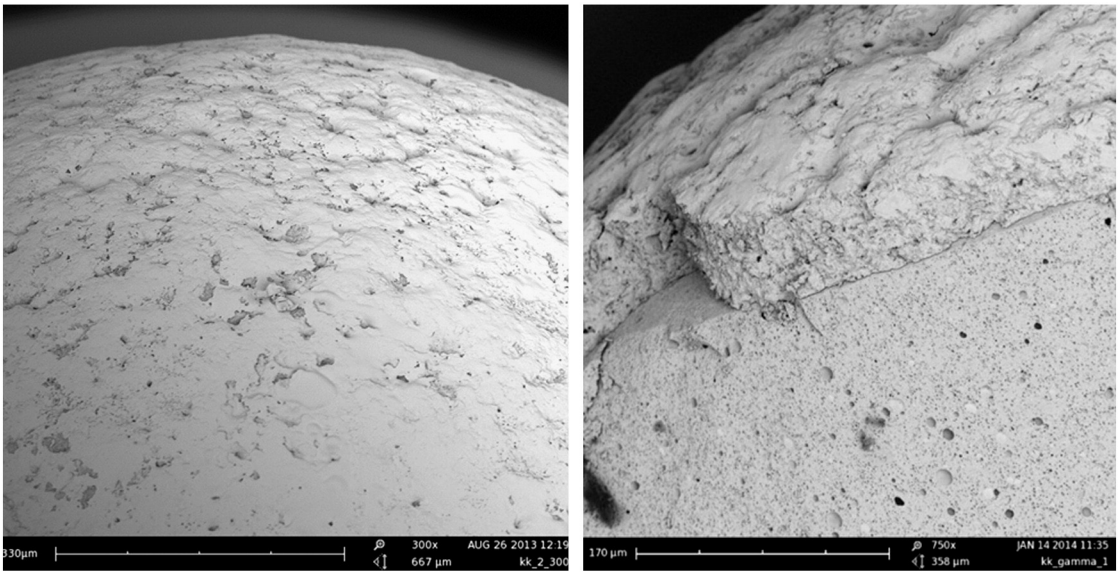

Fig. 13. SEM image of coating made of sodium benzoate with HPMC (0.5%); 60 °C gas inlet temperature, 600 g/h spraying rate.

with the average coating thickness of $s = 44.5$ µm from the single X-ray image (Table 5) in a coating layer porosity of $\varepsilon_c = 0.166$. Assuming that coating porosity is the same for all particles produced in the same batch and comparing with the porosity values of Table 4, shows that this value is quite realistic. Consequently, the short-cut method of non-tomographic X-ray irradiation can also be used to, indirectly, obtain coating layer porosities as long as the assumptions behind Eq. (1) are relatively well fulfilled, which seems to be the case for nearly spherical particles. However, if the particles are irregular in shape, then full µ-CT measurements need to be conducted in order to directly determine coating layer porosity.

4.5. Determination of average coating thickness of a particle population

The possibility to obtain fast and reliable measurement for the average coating thickness on a particle by evaluation of a single X-ray image allows investigation of the distribution of the average thickness in a particle population, i.e. large number of coated particles can be investigated in a limited amount of time. The time saving can be increased further if more particles are irradiated simultaneously at the same time. In a series of evaluations a number of particles, usually between six and eight, were fixed on a cardboard which was attached to a wire of known thickness. This construction, shown in Fig. 14, was then mounted on the sample holder.

For each set of particles, one X-ray image was obtained as described in the preceding section and in Table 5. The cumulative frequency distribution of the average coating thickness in the particle population produced by the spray fluidized bed experiment described in Section 2.1, based on a sample of 96 measured particles, is shown in Fig. 15. All obtained thickness values range from 39.6 µm to 48.8 µm, with an average layer thickness of 44.9 µm and a standard deviation of 2.52 µm in the particle population.

Table 5
Results of coating thickness, comparing single X-ray image with complete µ-CT measurements.

Measurement	Rotation steps [°]	Measuring time [hh:mm]	Voxel size [µm/px]	Average thickness [µm]
Single X-ray image	–	00:02	1.6	44.5
A1	0.225	01:45	1.6	44.6
A2	0.9	00:25	1.6	44.8

In pharmaceutical research, X-ray computed tomography and the optical coherence tomography are common methods to investigate internal structures of press-coated tablets or polymer coating structures, e.g. by Moweri et al. [23] Tokudome et al. [24], or by Li et al. [25]. It is, however, to the best of the authors' knowledge the first systematic study on reduction of time requirement of µCT measurements retaining the accuracy of coating layer measurements. It also presents for the first time a setup which allows the measurement of an average coating thickness distribution in a particle population by X-ray micro-tomography. This direct determination is much more reliable than comparison of particle size distributions for coated and uncoated particles, which is often done in industry by subdividing the cumulative distributions to the same number of size classes and assuming arbitrarily that coated particles of a certain class have resulted from the corresponding size class of uncoated particles. From the point of view of product quality, the resulting average coating layer

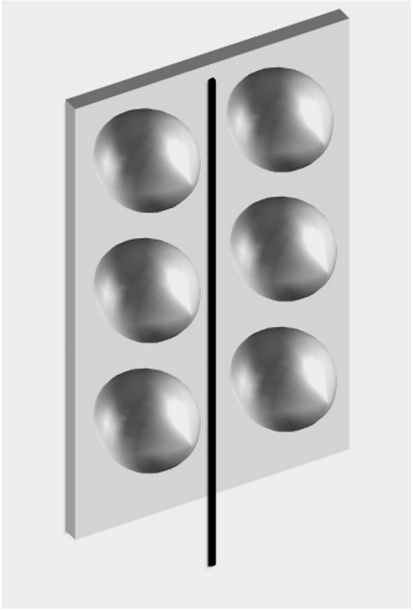

Fig. 14. Scheme of the construction of a sample holder for a set of particles.

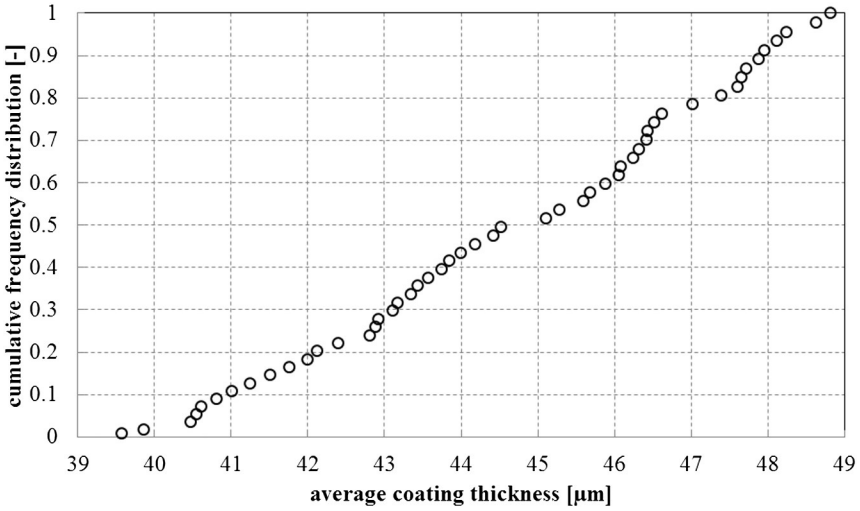

Fig. 15. Cumulative frequency distribution of average coating thickness in particle population.

distribution should be as narrow as possible, i.e. regardless of core size all particles should be coated by a layer of almost identical thickness.

5. Summary and conclusion

A study was conducted on the application of X-ray μ-computed tomography to measure the coating thickness on core particles (alumina) coated by sodium benzoate with some HPMC in a spray fluidized bed. Two different methods have been presented with which layer thicknesses can be determined. First, two-dimensional images were used, which were obtained after μ-CT measurements. In these measurements conditions like rotation steps and image averaging were tested to find the best suitable settings for high contrast and sharp images. A radial grid was overlaid on the obtained images. Along the radial lines, which were set manually, layer thickness values were measured. All average layer thickness values obtained in this way for one and the same coated particle were very close to each other. This means that coating layer thicknesses can be determined accurately even when using large rotation steps and refraining from image averaging.

The second presented method works by using single X-ray images, which are easier and much faster to achieve. Comparison has shown that layer thicknesses evaluated from single X-ray images without rotation match very well with thicknesses obtained by using two-dimensional images from complete μ-CT measurements with sample rotation. It has also been shown that this quick but accurate method can be used for the simultaneous investigation of several coated particles. This opens the way to the measurement of coating thickness distribution in a particle population, with great potential for practical application. Such measurement was not feasible before, because of the time and labor necessary to investigate a sufficiently large number of coated particles.

For the investigation of coating layer porosity, full μ-CT measurements were done with varied settings of image averaging and rotation steps. The obtained volume images are the base for the porosity investigation. Despite of some dependence on the chosen measurement setting, coating layer porosities were found to be sufficiently accurate and consistent with the measured coating thicknesses. In fact, it was shown that in case of spherical particles coating porosity needs not be measured, but can be calculated from the measured average coating thickness by means of Eq. (1). However, this cannot be done with irregularly shaped particles, so that full μ-CT measurements would be necessary for determination of coating porosity in that case.

An interesting side-result of the investigation concerns the effect of HPMC. Comparison with previous data obtained without addition of HPMC to the coating liquid (aqueous solution of sodium benzoate) has shown that even a small amount of HMPC results in a dramatic decrease of layer porosity, leading to quite compact and smooth coatings.

6. Outlook

Future investigations will apply the single X-ray image method to measure coating thickness distributions for particle populations produced at different operating conditions and in different types of spray fluidized bed equipment. Moreover, the application of X-ray μ-CT to coated particles of irregular shape shall be investigated. Finally, a systematic comparison of X-ray μ-CT with confocal laser scanning microscopy is planned. First experiments in this direction have been communicated by Sondej et al. [26] for similar process conditions and material compositions.

Acknowledgements

The authors gratefully acknowledge the funding of this work by: German Federal Ministry of Science and Education (BMBF) as part of the InnoProfileTransfer project NaWiTec (grant no. 03IPT701X); Forschungs-Gesellschaft Verfahrens-Technik (GVT), IGF project no. 17633 N; German Federal Ministry of Science and Education (BMBF) within the project WIGRATEC + (grant no. 03WKCI4A, 03WKCI4B); the X-ray micro tomographic device has been financed by the European Fund for Regional Development (EFRD, project no. 1211080002).

References

[1] M. Peglow, S. Antonyuk, M. Jacob, S. Palzer, S. Heinrich, E. Tsotsas, Particle formulation in spray fluidized bed, in: E. Tsotsas, A.S. Mujumdar (Eds.), Modern Drying Technology Volume 3: Product Quality and Formulation, Wiley-VHC Verlag GmbH & Co, KGaA, 2011, pp. 295–301.
[2] A. Bück, E. Tsotsas, K. Sommer, Size enlargement, in: B. Elvers (Ed.), Ullmann´s Encyclopedia of Industrial Chemistry, Wiley-VCH Verlag GmbH & Co, KgaA, 2014, pp. 1–47.
[3] R. Wesdyk, Y. Joshi, N. Jain, K. Morris, A. Newman, The effect of size and mass on the film thickness of beads coated in fluidized bed equipment, Int. J. Pharm. 65 (1–2) (1990) 69–76.
[4] M. Andersson, B. Holmquist, J. Lindquist, O. Nilsson, K.-G. Wahlund, Analysis of film coating thickness and surface area of pharmaceutical pellets using fluorescence microscopy and image analysis, J. Pharm. Biomed. Anal. 22 (2000) 325–339.
[5] F.L. Laksmana, P. Hartman Kok, H. Vromans, Quantitative image analysis for evaluating the coating thickness and pore distribution in coated small particles, Pharm. Res. 26 (4) (2009).
[6] P. Depypere, v. Oostveldt, J. Pieters and K. Dewettinck, Quantification of microparticle coating quality by confocal laser scanning microscopy (CLSM), Eur. J. Pharm. Biopharm. 73 (1) (2009) 179–186.

[7] C. Cahyadi, A. Karande, L. Chan, P.W. Heng, Comparative study of non-destructive methods to quantify thickness of tablet coatings, J. Pharm. Biopharm. 398 (1–2) (2010) 39–49.
[8] S. Sasic, Determining the coating thickness of tablets by chiseling and image analysis, Int. J. Pharm. 397 (1–2) (2010) 109–115.
[9] D. Koller, G. Hannesschläger, M. Leitner, J. Khinast, Non-destructive analysis of tablet coatings with optical coherence tomography, Eur. J. Pharm. Sci. 44 (1–2) (2011) 142–148.
[10] S. Zhong, Y.-C. Shen, L. Ho, R. May, J. Zeitler, M. Evans, P. Taday, M. Pepper, T. Rades, K.C. Gordon, R. Müller, P. Kleinebudde, Non-destructive quantification of pharmaceutical tablet coatings using terahertz pulsed imaging and optical coherence tomography, Opt. Lasers Eng. 49 (3) (2011) 361–365.
[11] I.-S. Russe, D. Brock, K. Knop, P. Kleinebudde, J. Zeitler, Validation of terahertz coating thickness measurements using X-ray microtomography, Mol. Pharm. 9 (12) (2012) 3551–3559.
[12] G. Farber, Tardos and J. Michaels, Use of X-ray tomography to study the porosity and morphology of granules, Powder Technol. 132 (2003) 57–63.
[13] B. Hancock, M. Mullarney, X-ray microtomography of solid dosage forms, Pharm. Technol. (2005) 92–100.
[14] J. Zeitler, L. Gladden, In-vitro tomography and non-destructive imaging at depth of pharmaceutical solid dosage forms, Eur. J. Pharm. Biopharm. 71 (1) (2008) 2–22.
[15] G. Perfetti, E. v. d. Casteele, B. Rieger, W. Wildeboer and G. Meesters, X-ray micro tomography and image analysis as complementary methods for morphological characterization and coating thickness measurement of coated particles, Adv. Powder Technol. 21 (6) (2010) 663–675.
[16] M. Dadkhah, M. Peglow, E. Tsotsas, Characterization of the internal morphology of agglomerates produced in a spray fluidized bed by X-ray tomography, Powder Technol. 228 (2012) 349–358.
[17] N. Hampel, A. Bück, M. Peglow, E. Tsotsas, Continuous pellet coating in a Wurster fluidized bed process, Chem. Eng. Sci. 86 (2013) 87–98.
[18] M. Dadkhah, Morphological characterization of agglomerates produced in a spray fluidized bed by X-ray tomography, Magdeburg, Dissertation, docupoint Verlag, 2014.
[19] L. Wojnar, Image analysis: application in material engineering, CRC Press, Boca Raton, USA, 1999.
[20] N. Hampel, Diskontinuierliches und kontinuierliches Pelletcoating im Wurster-Wirbelschichtprozess, Dissertation, Magdeburg, 2014.
[21] M. Peglow Hoffmann, E. Tsotsas, Influence of process parameters on the particle surface in fluidized bed spray granulation, 18th International Drying Symposium, Xiamen, China, 2012.
[22] C. Rieck, T. Hoffmann, A. Bück, E. Tsotsas, Influence of drying conditions on coating layer porosity in fluidized bed spray granulation, Powder Technol. 272 (2015) 120–131.
[23] M.D. Moweri, R. Sing, J. Kirsch, A. Razaghi, S. Béchard, R.A. Reed, Rapid at-line analysis of coating thickness and uniformity on tablets using laser induced breakdown spectroscopy, J. Pharm. Biomed. Anal. 28 (5) (2002) 935–943.
[24] Y. Tokudome, H. Ohshima, M. Otsuka, Non-invasive and rapid analysis for observation of internal structure of press-coated tablet using X-ray computed tomography, Drug Dev. Ind. Pharm. 35 (6) (2009) 678–682.
[25] C. Li, A. Zeitler, Y. Dong, Y.-C. Chen, Non-destructive evaluation of polymer coating structures on pharmaceutical pellets using full-field optical coherence tomography, J. Pharm. Sci. 103 (2014) 161–166.
[26] F. Sondej, A. Bück, E. Tsotsas, Experimental analysis of the micro-structure of single particles and micro-droplets, in 19th International Drying Symposium, Lyon, France, 2014.